

## CHAPTER 222

### Sediment Transport in Dredged Trenches

S. Opatha Vithana\*, MICE(Lond.), MIEAust.

#### Abstract

An attempt was made, using a 3-dimensional turbulent model coupled with a comparatively simple depth averaged sand transport model, to assess the computational feasibility of predicting sediment transport in a dredged trench, caused by a steady flow passing across the trench. A sophisticated computer software package was used to simulate 3-dimensional turbulent flow by the finite element method. A Profile Model, which discretized the transport process to enable successive computation of the flow field, was used for morphological evolution of the channel bed. A physical model was built and tested to validate the numerical models.

#### 1.0 Introduction

An attempt to set up a mathematical theory of sedimentation should take into account both the character of the fluid motion and character of the sediment motion. The K-Epsilon model is considered as the best mathematical model available at present to represent turbulent flow. Any mathematical model to represent sediment transport should take into account the movement of sediment by both suspension and bed load. Movement of sediment in suspension is considered to be best described by the diffusion-convection equation. Therefore, if K-Epsilon model is coupled with the diffusion-convection equation together with a bed load formula one can expect a very good mathematical model to represent sediment transport. However, for long term morphological computations implying the successive computation of the flow field, the use of K-Epsilon model or the diffusion-convection equation is still not attractive because of the limitations of available computer resources. To overcome this problem various mathematical models have been proposed by combining the simplified diffusion-convection equation with comparatively simple flow models.

In this paper an attempt made to assess the computational feasibility of solving this complex problem by using a

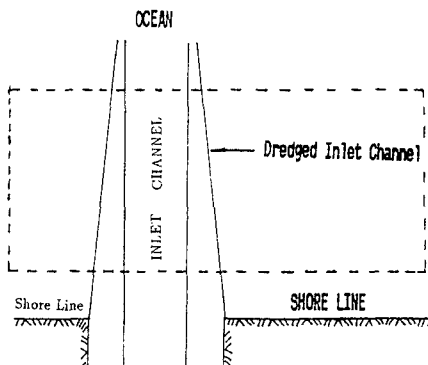
---

\* Superintending Civil Engineer, Sri Lanka Ports Authority, Colombo-1, Sri Lanka.

3-dimensional turbulent model coupled with a comparatively simple sand transport model is presented.

2.0 Physical Model

A physical model of the entry to a dredged navigational channel through a shelving coastline was built to simulate siltation effects. The flow and siltation conditions obtained from the physical model were used to verify the two numerical models which were under assessment.



The plan view of the inlet area considered for study is the area enclosed by broken lines in Fig. 1.0. Dimensions and isometric view of the flow domain are shown in fig.2.0.

Fig. 1.0: Area Considered for Detailed Study.

The slope of the bed in the transverse direction represents the gradient of the sea bed in the shore region.

The bed consisted of fine to medium sand of almost uniform size with the characteristic diameters of:  $d_{10} = 150 \mu\text{m}$ ,  $d_{50} = 240 \mu\text{m}$ , and  $d_{90} = 380 \mu\text{m}$ . A continuous steady flow with a mean flow velocity of about 0.3 m/sec, which was considered to be large enough to initiate movement of the sediment used in the experiment, was maintained into the model during the experiment.

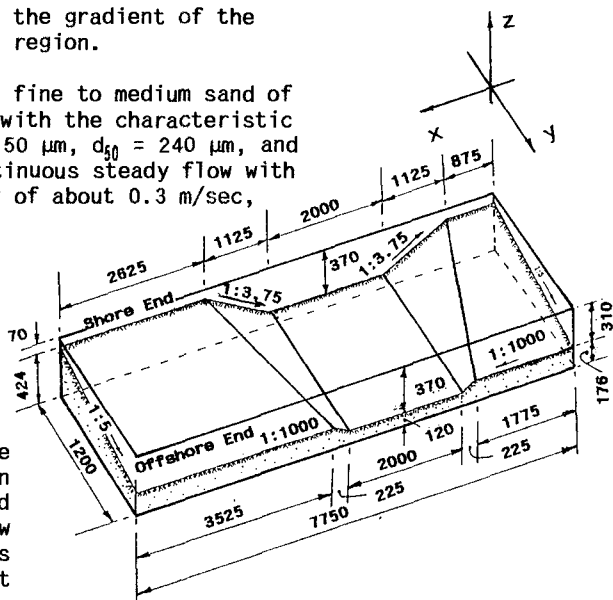


Fig.2.0: Isometric View of the Flow Domain.

For validation of the flow simulation model, inlet and downstream flow velocity measurements should be carried out on a fixed bed model.

Therefore, at the first instance, the entire bed of the physical model was covered with steel sheets to maintain a fixed bed and all flow velocity measurements were carried out using Laser-Doppler velocity measuring equipment. In order to obtain input velocity boundary conditions for the flow simulation model, inlet velocity components in longshore and offshore

directions were measured on all finite element grid lines. For calibration of the flow simulation model, measurement of the longshore velocity components were carried out at four different downstream sections, at  $x = 1.75, 3.0, 4.5$  and  $7.25$  meters.

When calibration of the flow simulation model was completed, the metal sheets used to cover the bed were removed and the flow was restarted to validate the sand transport model. After 6.0 hrs. of continuous steady flow, the flow was discontinued and the bed profiles of the entire area under consideration was measured.

### 3.0 Numerical Models

#### 3.1 Flow Simulation Models

A general purpose computer software package (FIDAP) which uses the finite element method to simulate many classes of incompressible fluid flows was used to simulate turbulent flow across the channel. In FIDAP the three-dimensional, steady, turbulent flow of an incompressible viscous fluid is represented by the following equations:

$$- \text{Mass Conservation; } \frac{\partial u_j}{\partial x_j} = 0$$

$$- \text{Momentum Conservation; } u_j \frac{\partial u_i}{\partial x_j} = - \frac{\partial p}{\partial x_i} + \frac{\partial}{\partial x_j} \left[ \mu \left( \frac{\partial u_i}{\partial x_j} + \frac{\partial u_j}{\partial x_i} \right) \right]$$

where,  $u_j$  = mean fluid velocity component,  $p$  = fluid pressure,  $x_j$  = cartesian coordinates,  $i = 1,2,3$ ,  $j = 1,2,3$ ,  $\mu$  = total viscosity =  $\mu_0 + \mu_t$ ,  $\mu_0$  = laminar viscosity,  $\mu_t$  = turbulent viscosity.

Two possible turbulent models are available in FIDAP to determine the distribution of turbulent viscosity (or eddy viscosity).

##### 3.1.1 K-Epsilon Model

The three-dimensional version of the K-Epsilon model comprises three additional equations as indicated below:

$$\rho u_j \frac{\partial K}{\partial x_j} = \frac{\partial}{\partial x_j} \left( \frac{\mu_t}{\sigma_K} \frac{\partial K}{\partial x_j} \right) - \rho \epsilon$$

$$\rho u_j \frac{\partial \epsilon}{\partial x_j} = \frac{\partial}{\partial x_j} \left( \frac{\mu_t}{\sigma_\epsilon} \frac{\partial \epsilon}{\partial x_j} \right) - \rho C_2 \frac{\epsilon^2}{K}$$

$$\mu_t = \rho C_\mu \frac{K^2}{\epsilon}$$

FIDAP adopts the Galerkin form of the weighted residuals method to solve these differential equations by the finite element method.

##### 3.1.2 Mixing Length Model

In the mixing length model, the turbulent viscosity is represented by the Prandtl mixing length hypothesis.

$$\mu_t = \rho l_m^2 \left[ \left( \frac{\partial u_i}{\partial x_j} + \frac{\partial u_j}{\partial x_i} \right) \frac{\partial u_i}{\partial x_j} \right]^{1/2}$$

In FIDAP the mixing length values are computed based on Nikuradse's (Rodi W., 1980) Formula:

$$\frac{l_m}{R} = 0.14 - 0.08 \left(1 - \frac{y}{R}\right)^2 - 0.06 \left(1 - \frac{y}{R}\right)^4$$

where, R = depth of flow, y = normal distance from the wall.

### 3.1.3 Boundary Conditions for Flow Simulation Models

#### 3.1.3.1 Inlet Boundary

Mean velocities of flow in all three coordinate directions (u,v,w), turbulent kinetic energy (K), and its dissipation rate ( $\epsilon$ ) should be specified at the inlet.

##### (a). Mean Flow Velocities

Inlet velocity components in the longshore and offshore directions measured in the physical model were prescribed as input to the numerical model. Inlet velocity in the vertical direction was assumed to be zero.

##### (b). Turbulent Kinetic Energy

Time-averaged values of the fluctuating components of the fluid velocities  $\bar{u}'$  and  $\bar{v}'$  measured at the inlet by the Laser-Doppler equipment were used in calculating the turbulent kinetic energy (K) at the inlet, using the formula:

$$K = \frac{1}{2} [(\bar{u}')^2 + (\bar{v}')^2 + (\bar{w}')^2]$$

The prescribed initial values of K and  $\epsilon$  at the inlet seems to exert little influence on the predictive accuracy of the flow simulation models (Leschziner M.A., et al. 1979). Therefore, as velocity measurements were not carried out in the vertical direction it was assumed that,  $\bar{w}' = \bar{u}'$ .

##### (c). Dissipation Rate of Turbulent Kinetic Energy

Dissipation rate of turbulent kinetic energy ( $\epsilon$ ) was evaluated from the following formula (Lauder B.E., et al. 1974) using the values of measured turbulent kinetic energy (K).

$$\epsilon = \frac{C_\mu^{3/4} K^{3/2}}{l_m} ; \text{ in which } l_m \text{ is a mixing length}$$

It was assumed that the value of mixing length is given by the well-known ramp function for wall boundary layers (Lauder B.E., et al. 1972):

$$l_m = \lambda y_G$$

where,  $\lambda$  = a constant in mixing length model,  
 $y_G$  = effective width of shear flow.

The characteristic shear width of flow was calculated using the

measured inlet velocity profiles (Lauder B.E., et al. 1972). A value of 0.125 was assumed for  $\lambda$ .

### 3.1.3.2 Wall Boundaries

The variation of the turbulent viscosity within the viscous sublayer in the near-wall region was modelled using van Driest's mixing length model with a transition to the standard high Reynolds number K-Epsilon model in flow region beyond the viscous sublayer where the turbulence is fully developed. In the van Driest mixing length approach, the eddy viscosity is defined as described in Section 3.1.2 and the van Driest mixing length is defined as,

$$l_m = k \delta (1 - e^{-y_{\text{eff}}^*/A})$$

where, A = an empirical constant, k = von Karman constant,  $\delta$  = normal distance from the wall.

In this equation  $y_{\text{eff}}$  is the dimensionless normal distance from the wall defined in terms of the turbulent kinetic energy as,

$$y_{\text{eff}}^* = \rho \delta \frac{(c_\mu^{1/2} K)^{1/2}}{\mu}$$

where,  $c_\mu$  = a turbulent constant,  $\mu$  = dynamic viscosity, K = turbulent kinetic energy.

While the computational domain for the mean flow equations encompasses the flow domain up to the solid boundary, the corresponding computational domain for the K- $\epsilon$  turbulent model only extends to near wall region. As part of near-wall implementation, FIDAP applies the following boundary conditions for K and  $\epsilon$ .

$$\frac{\partial K}{\partial n} = 0 ; \quad \epsilon = \frac{(c_\mu^{1/2} K)^{1.5}}{k \delta}$$

where, n is the direction normal to the boundary.

If no-slip boundary condition is valid at the wall, then all the velocity components assume a zero value at the wall.

### 3.1.3.3 Outlet Boundary

The outlet boundary was located far away from the area of interest so as to allow the redevelopment of fully developed flow downstream. At the outflow no velocity boundary conditions were imposed, resulting in zero normal and tangential stresses at the outflow boundary. Similarly, the turbulent kinetic energy and dissipation were not specified at the outflow boundary.

### 3.1.3.4 Water Surface

The position of the free water surface was assumed to be fixed and at the free water surface the velocity component in the vertical direction was assumed to be zero.

### 3.1.4 Creating Finite Element Mesh

The three-dimensional flow domain was first divided into a set

of 8 node brick elements. All wall boundaries were divided into quadrilaterals with 4 nodes. As the computation time needed to solve the equations is large for a finer mesh, a compromise had to be made between the accuracy and the computation time before selecting the following dimensions.

The longitudinal direction was divided into 31 elements of length 250 mm each and the transverse direction consisted of 8 elements of width 150 mm each. The vertical direction consisted of 8 elements, the dimensions of which were decreased towards the bed to provide a greater resolution in the zone where large velocity gradients exist. The solution domain thus consisted of 1984 brick elements of 8 nodes each and 2592 nodal points.

3.1.5 Fluid Properties

Following data was used as the physical properties in the flow simulation models.

fluid density,  $\gamma = 1000.0 \text{ kg/m}^3$ ; kinematic viscosity,  $\nu = 1 \times 10^{-6} \text{ m}^2/\text{sec}$ ; turbulence constant,  $c_{\mu} = 0.09$ ; empirical constants:  $c_{1E} = 1.44$ ,  $c_{2E} = 1.92$ ,  $\sigma_k = 1.00$ ,  $\sigma_\epsilon = 1.30$ ; von Karman constant,  $k = 0.41$ ; van Driest's constant,  $A = 26.00$ .

3.2 Sand Transport Model

The model considered was basically similar to what was used by Hillier and Jenkins (1976). As shown in Figure 3.0, the model zone was divided into a grid system on the horizontal plane, the longshore and offshore directions being divided into equal number of sections as used in the mesh for flow simulation models.

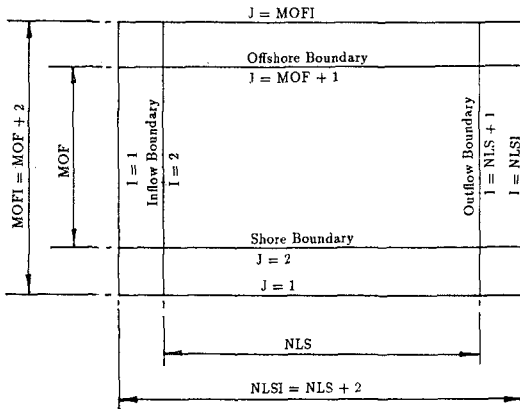


Fig. 3.0: Grid System of the Sand Transport Model

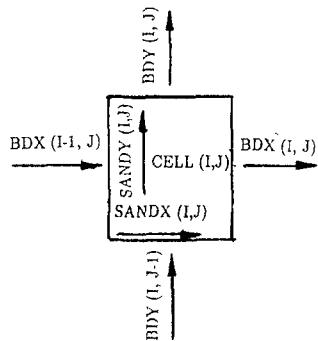


Fig. 4.0: Sediment Transport in a Cell

- MOF = number of cells in the offshore direction = 8
- NLS = number of cells in the longshore direction = 31

For the purpose of comparison, two different formulae were used to calculate the sand transport. In the first method, Shield's (1936) bedload formula and in the second method a new approach to calculate sediment transport by Ackers and White (1973) was used.

### 3.2.1 Shield's Formula

Shield's Bedload Formula for calculation of sand transport can be written as follows:

$$\frac{q_s \gamma_s}{q S \gamma} = 10 \frac{\tau_0 - (\tau_0)_{cr}}{(\gamma_s - \gamma) d}$$

where;  $q_s$ ,  $q$  = rate of bedload and liquid in volume per unit time and unit width respectively,  $S$  = slope of the energy grade line,  $\gamma$  = specific weight of liquid,  $\gamma_s$  = specific weight of sediment,  $\tau_0$  = shear stress,  $(\tau_0)_{cr}$  = critical shear stress at which sediment particles are about to move,  $d = d_{50}$  = mean particle diameter.

The rate of liquid flow can be related to the mean flow velocity as:  $q = V \times H$ ; in which,  $V$  = mean flow velocity,  $H$  = depth of flow.

The bed shear stress can be calculated from (2),  $\tau_0 = \gamma H S$ ; the critical bed shear stress, ( $\text{kg/m}^2$ ), can be related to the mean particle diameter (meters) as (Kalinske A.A.),  $(\tau_0)_{cr} = 192.65 d$ .

The slope of the energy grade line can be expressed in metric units (for manning's  $n = 0.025$ ) as (Graf W.H., 1971),

$$S = \frac{0.0006 \times V^2}{H^{4/3}}$$

Substitution of these values along with  $\gamma_s = 2650.0 \text{ kg/m}^3$  in Shield's Formula will finally yield:

$$q_s = 0.0057 \frac{V^3}{H^{1/3}} [0.59723 \frac{V^2}{H^{1/3}} - 0.04624]$$

Therefore when the values of  $V$  and  $H$  are known, the sediment transport can be calculated using the above equation.

### 3.2.2 Method Proposed by Ackers and White

Ackers and White (1973) has proposed a method to calculate transport of non-cohesive sediment by a steady uniform flow. When the physical properties of the fluid and sediments are substituted, the value of  $S$  is expressed as in Section 3.2.1, and shear velocity is defined as  $v_* = \sqrt{gHS}$ , sediment transport rate can finally be expressed in terms of  $V$  and  $H$  as follows:

$$q_s = 1.2567 \times 10^{-5} \cdot v \cdot H^{0.0936}$$

$$\left[ \frac{7.7019 v}{H^{0.0936} [\log_{10}(4.1667 \times 10^{-4} H)]^{0.4382}} - 1 \right]^{2.9343}$$

Therefore, when the values of the mean velocity ( $V$ ) and the mean

depth of flow (H) are known the sediment transport can be calculated using the above equation.

### 3.2.3 Calculation of Sediment Transport Rate

For calculation of sediment transport rate, depth averaged velocities were used in the sand transport formula. Therefore, the nodal velocities obtained from the flow simulation model were first converted to depth averaged nodal velocities. These depth averaged nodal velocities were then converted to cell velocities in the longitudinal and transverse directions. Using the Sand transport formula, the rate of sediment transport was calculated in longitudinal and transverse directions for each cell.

With reference to Figure 4.0, SANDX(I,J) and SANDY(I,J) are defined as rates of sand transport in Cell (I,J) in x & y directions respectively. If just one cell is considered its sediment transport components can be averaged with those of the surrounding cells to obtain the boundary flow.

$$\begin{aligned} \text{Boundary flow in longitudinal direction} &= \text{BDX}(I,J) \\ &= 1/2.[\text{SANDX}(I,J) + \text{SANDX}(I+1,J)] \\ \text{Boundary flow in transverse direction} &= \text{BDY}(I,J) \\ &= 1/2.[\text{SANDY}(I,J) + \text{SANDY}(I,J+1)] \end{aligned}$$

The sand movement within the cell is then the difference between the transport rates into the cell and the transport rates out of the cell.

$$\begin{aligned} \text{Net longitudinal sand transport in cell}(I,J) &= \text{XMOVE}(I,J) \\ &= \text{BDX}(I-1,J) - \text{BDX}(I,J) \\ \text{Net transverse sand transport in cell}(I,J) &= \text{YMOVE}(I,J) \\ &= \text{BDY}(I,J-1) - \text{BDY}(I,J) \end{aligned}$$

The sediment movement is actually a volume rate per unit time per unit width. Therefore, multiplication by the cell width and an appropriate time interval will yield the volume change of sand. Then simply dividing by the cell area will give the change in depth of the cell.

$$\begin{aligned} \text{The amount of Erosion or Deposition in cell}(I,J) &= \text{RISE} \\ &= [\text{M.XMOVE}(I,J) + \text{N.YMOVE}(I,J)].\text{MTA}/\text{AREA} \end{aligned}$$

where, M,N = width of cell(I,J) in transverse and longitudinal directions respectively, AREA = M x N, MTA = time period for which the sand transport is calculated.

$$\text{New Depth of Cell}(I,J) = H(I,J) - \text{RISE}$$

### 3.2.4 Boundary Conditions for the Sand Transport Model

Following boundary conditions were used in the Sand Transport model.

#### 3.2.4.1 Inflow Boundary

At the inflow boundary it was assumed that the rate of sediment transport in longitudinal direction was equal to the rate of sediment

transport in the first cell in the same direction, figure 3.0.

$SANDX(I,J) = SANDX(2,J)$  and  $H(1,J) = H(2,J)$ ; where,  $J = 2$  to  $MOF+1$

#### 3.2.4.2 Outflow Boundary

At the outflow boundary the rate of sediment transport in longitudinal direction was assumed to be equal to the rate of sediment transport in the last cell in the same direction.

$SANDX(NLSI,J) = SANDX(NLS+1,J)$  ,  $H(NLSI,J) = H(NLS+1,J)$   
where,  $J = 2$  to  $MOF+1$

#### 3.2.4.3 Shore Boundary

At the shore boundary, the rate of sediment transport in the transverse direction was assumed to be zero.

$SANDY(I,1) = 0.0$  and  $H(I,1) = H(I,2)$ ; where,  $I = 2$  to  $NLS+1$

#### 3.2.4.4 Offshore Boundary

Similar to the shore boundary, the rate of sediment transport in the transverse direction was assumed to be zero.

$SANDY(I,MOFI) = 0.0$  and  
 $H(I,MOFI) = H(I,MOF+1)$  where,  
 $I = 2$  to  $NLS+1$

### 3.3 Profile Model

Using a flow simulation model described in Section 3.1 and a sand transport model described in Section 3.2 a Profile Model, as shown in the Flow Chart in Figure 5.0, was developed for morphological evolution of the shore area.

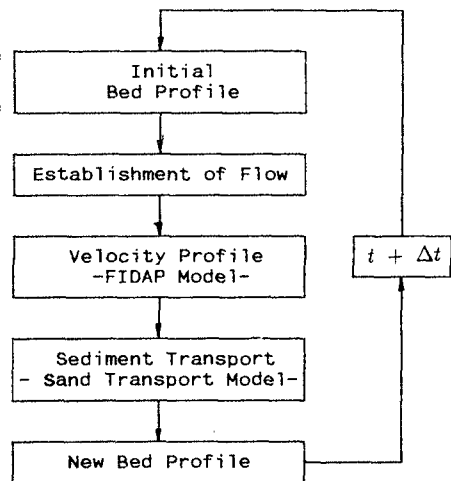


Figure 5.0: Flow Chart of the Profile Model

The constituents of the Profile Model are as follows:

- The initial bed profile of the area under consideration is decided.
- A known flow field is established over the area under consideration.
- The velocity field in the computation domain is numerically simulated using Mixing Length Model.
- Rate of transport of sediment due to known velocity field is calculated using the Sand Transport Model.
- Change of bed profile due to transport of sediment for a time period  $\Delta t$  is calculated and the new bed profile is obtained.

The new bed profile obtained after time  $\Delta t$  was used as the initial profile for the next cycle. This procedure was continued until

sufficient number of cycles are completed over the required time period for which morphological evolution of the shore area is to be determined.

4.0 Results and Discussion

4.1 Flow Simulation Models

Computed velocity profiles using the K-Epsilon and Mixing Length models have been compared against the measured velocities, at four different sections, in Figure 6.0.

It was observed that the K-Epsilon model, in general, predicted velocities closer to the measured values when compared to the Mixing Length Model. Specially, in the flow velocity measuring stations downstream of the dredged channel, ie. at  $x = 4.5$  and  $x = 7.5$  m, the K-Epsilon Model predicted velocities to a fairly good accuracy.

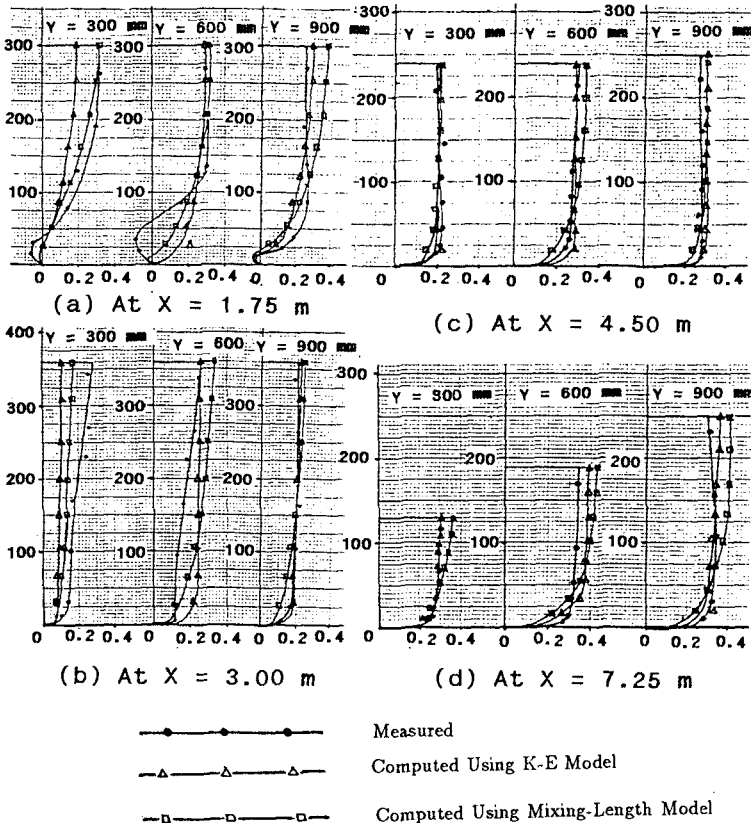


Figure 6.0: Measured and Computed Velocities

However, it was observed that the computed velocities deviated

from the measured velocities in the region from the inlet upto the dredged channel. When the cause for this situation was examined it was observed that selected inlet section was too close to the dredged channel. However, limited space available in the Hydraulic Laboratory did not allow shifting of the inlet section further upstream of the dredged channel.

The following assumptions made in making the numerical models would also have affected the accuracy of the predicted results.

- \* All wall boundaries, including the bed boundary, have been assumed to be fully rough (no-slip boundary condition.)
- \* For specification of normal and tangential boundary condition, the bed boundary has been assumed to be horizontal.

It is also expected that accuracy of computed velocities could be increased by having a finer mesh discretization, specially in the recirculation region.

Therefore, it can be concluded that under assumed conditions flow simulation models gave reasonable to good accuracy except for a few sections in the recirculation and inlet regions which in retrospect would have been expected.

## 4.2 Sand Transport Models

### 4.2.1 Shield's Formula

Shield's formula which is essentially a bed load formula is based on the assumption that shear stress is the main parameter defining sediment transporting power. Transport of sediment by suspension at higher shear velocities has not been taken into account and at all velocities sediment is assumed to be transported as bed load. Further, the resistance to sand movement caused by the bed forms on the deformed bed has not been considered in the formula.

The velocity field existing at the granular surface determines the shear stress on the grains. Therefore, it is more realistic to relate the bed shear velocity to the flow velocity at the bed level. But in this experiment, the bed shear stress, hence the bed shear velocity, in the Shield's formula has been related to the depth averaged mean flow velocity which could be higher than the near bed velocity.

Due to these reasons and also since the sand transport is a function to the fifth power of the mean fluid velocity (Section 3.2.1) exaggerated sand movement can be expected in areas where the velocity is high relative to the depth.

Examination of bed profiles at the inlet region showed that predicted higher velocities have caused exaggerated erosion and deposition of the cells in the region and the model became unstable after few iterations.

As Shield's formula is purely a bed load formula, errors in predicted results can be expected at higher shear velocities relative to the critical shear velocity. Therefore, Shield's formula was not considered as suitable for long term morphological computations.

#### 4.2.2 Ackers and White Method

This method predicts the total load and not the bed-load transport only. In this method average stream velocity has been used in preference to shear stress as the basis of sediment transport function. The grain roughness has been taken into account by relating it to the median sediment diameter. As such this method can be expected to perform better than the Shield's formula.

The following observations can be made when the bed contours, as shown in Fig. 8 and bed profiles shown in Fig. 7, are reviewed.

1. A prominent movement of sand in the longshore direction was seen throughout the flow domain; a clear overprediction compared to the Physical Model.

2. In the area downstream of the dredged channel where the computed and measured flow velocities had a better match, measured and computed bed profiles and contours have similar shapes and are almost parallel.

3. The movement of sand in the offshore direction observed in the Physical Model was not seen in the numerical model. This can not be explained in terms of flow velocities as both measured and computed flow velocities in offshore direction were small compared to the longitudinal

velocities. It should be noted here that the effect of gravity has not been taken into consideration in the numerical model. As such it will be interesting to examine whether the gravity has played a role in the movement of sand along the steep gradient in the transverse direction.

4. In the upstream region of the dredged channel where the computed

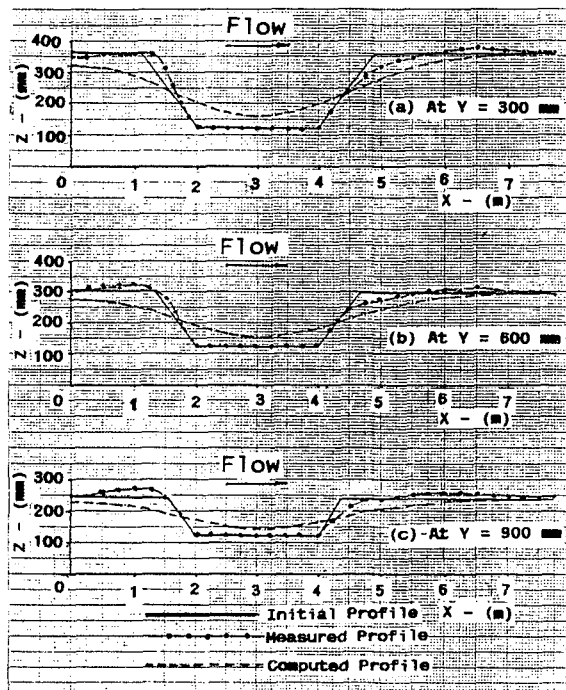


Fig. 7.0: Measured and Computed Bed Profiles

(Mixing Length Model) velocities did not show a good agreement with the measured velocities, the computed bed profiles deviated from the measured profiles as would be expected.

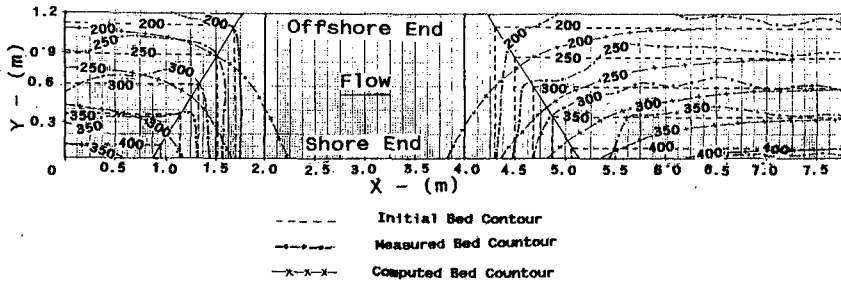


Fig. 8.0: Measured and Computed Bed Contours

An important factor that would have affected the predictions of the sand transport model is the changing bed profile and hence the flow velocities at the inlet which has not been taken into consideration. It was assumed that the prescribed inlet velocities remain unchanged throughout the experiment even though the bed profile was allowed to vary. As the computed flow velocities upstream of the dredged channel were found to be very sensitive specially to the direction and the magnitude of transverse velocities, this would have had a direct effect on the model predictions.

#### 4.3 Conclusions

The sand transport model which used the Ackers and White method performed reasonably well in the areas where the computed velocities were in agreement with the measured velocities. As the sand transport is a function to the fourth power of the mean velocity, (Section 3.2.2), a small error in the predicted flow velocities could accumulate to create a major error in the predictions of the sand transport model when a simulation is carried out over a large number of cycles for long term morphological computations. Thus, the accuracy of predictions of such a long term model will depend critically upon the accuracy of the predicted velocities in the flow simulation model.

It can be concluded that, once calibrated and validated using measured data, an advanced flow simulation model coupled with a simple sand transport model, as used in this experiment, appears feasible at this stage to predict long term morphological computations to a reasonable accuracy.

#### 4.4 Future Work

Since the numerical models performed reasonably well even without improvement, it would be worthwhile to investigate the influence of the factors such as; proximity of the inlet section to the dredged channel, change of cross-section at the inlet, a refined mesh, and influence of gravity, etc. on the performance of the models.

The sand transport model used looks crude compared to the advanced flow models used. However, as this is only the first developmental model better sand transport models can be coupled with the flow model to improve the predictions.

#### 4.5 Acknowledgements

The research project mentioned in this paper was carried out by the author when reading for a degree of Master of Engineering Science at the University of Adelaide, Australia under the supervision of Mr. R.Culver, Hon. Visiting Research Fellow. Thanks are due to the Australian International Development Assistance Bureau for the award of the research scholarship. The financial support for the hire of the commercial computer software package by the Department of Civil Engineering is acknowledged. The author is indebted to the individuals who have helped by various means in this study.

#### References

1. Ackers, Peter, and White, W.R. (1973). "Sediment Transport: New Approach and Analysis". *Journal of the Hydraulics Division*, Vol.99, No.HY11, pp.2041-2060.
2. Graf, W.H. (1971). *Hydraulics of Sediment Transport*. Mc Graw-Hill Book Company.
3. Hiller, M.E., and Jenkin, R.D. (1976). *Digital Coastal Outflow Simulation*. University of Adelaide, Australia.
4. Kalinske, A.A. "Movement of Sediment as Bedload in Rivers". *Transactions of the American Geophysical Union*. Vol.28, No.4, pp.616-620.
5. Launder, B.E., Morse, A., Rodi, W., and Spalding, D.B. (1972). "Prediction of Free Shear Flows - A Comparison of the Performance of Six Turbulence Models". *Proceedings of NASA*. pp.361-414.
6. Launder, B.E., and Spalding, D.B. (1974). "The Numerical Calculation of Turbulent Flows". *Computer Methods in Applied Mechanics and Engineering*. Vol.3, pp.269.
7. Leschziner, M.A., and Rodi, W. (1979). "Calculation of Strongly Curved Open Channel Flow". *Journal of the Hydraulics Division*. ASCE, Vol.105, HY10, pp. 1297-1313.
8. Rodi, W. (1980). "Turbulence Models and Their Application in Hydraulics". *IAHR Section on Fundamentals*. Delft, The Netherlands.
9. Schields, A. (1936). "Anwendung der Aehnlichkeitsmechanik und der Turbulenz-forschung auf die Geschiebebewegunu". *Mitteilungen der reussischen Versuchsanstalt fur Wasserbau und Schiffbau*, Berlin, Germany, Vol.26.

The sand transport model used looks crude compared to the advanced flow models used. However, as this is only the first developmental model better sand transport models can be coupled with the flow model to improve the predictions.

#### 4.5 Acknowledgements

The research project mentioned in this paper was carried out by the author when reading for a degree of Master of Engineering Science at the University of Adelaide, Australia under the supervision of Mr. R.Culver, Hon. Visiting Research Fellow. Thanks are due to the Australian International Development Assistance Bureau for the award of the research scholarship. The financial support for the hire of the commercial computer software package by the Department of Civil Engineering is acknowledged. The author is indebted to the individuals who have helped by various means in this study.

#### References

1. Ackers, Peter, and White, W.R. (1973). "Sediment Transport: New Approach and Analysis". *Journal of the Hydraulics Division*, Vol.99, No.HY11, pp.2041-2060.
2. Graf, W.H. (1971). *Hydraulics of Sediment Transport*. Mc Graw-Hill Book Company.
3. Hiller, M.E., and Jenkin, R.D. (1976). *Digital Coastal Outflow Simulation*. University of Adelaide, Australia.
4. Kalinske, A.A. "Movement of Sediment as Bedload in Rivers". *Transactions of the American Geophysical Union*. Vol.28, No.4, pp.616-620.
5. Launder, B.E., Morse, A., Rodi, W., and Spalding, D.B. (1972). "Prediction of Free Shear Flows - A Comparison of the Performance of Six Turbulence Models". *Proceedings of NASA*. pp.361-414.
6. Launder, B.E., and Spalding, D.B. (1974). "The Numerical Calculation of Turbulent Flows". *Computer Methods in Applied Mechanics and Engineering*. Vol.3, pp.269.
7. Leschziner, M.A., and Rodi, W. (1979). "Calculation of Strongly Curved Open Channel Flow". *Journal of the Hydraulics Division*. ASCE, Vol.105, HY10, pp. 1297-1313.
8. Rodi, W. (1980). "Turbulence Models and Their Application in Hydraulics". *IAHR Section on Fundamentals*. Delft, The Netherlands.
9. Schields, A. (1936). "Anwendung der Aehnlichkeitsmechanik und der Turbulenz-forschung auf die Geschiebebewegung". *Mitteilungen der reussischen Versuchsanstalt fur Wasserbau und Schiffbau*, Berlin, Germany, Vol.26.